Tethys, 5, 13–24, 2008
Journal of Weather & Climate of the Western Mediterranean
www.tethys.cat
ISSN-1697-1523
eISSN-1139-3394
DOI:10.3369/tethys.2008.5.02

Journal edited by **ACAM**
(Associació Catalana de Meteorologia)

Conditioned climatology for stably stratified nights in the Lleida area

D. Martínez[1], J. Cuxart[1] and J. Cunillera[2]

[1]Meteorology group, Physics department, Universitat de les Illes Balears. Cra. Valldemossa, km. 7.5, 07122, Palma de Mallorca
[2]Servei Meteorològic de Catalunya (Meteocat)

Received: 21-V-2008 – Accepted: 10-IX-2008 – **Translated version**

Correspondence to: dani.martinez@uib.cat

Abstract

Nights with clear skies and weak winds are common in the western Mediterranean area when pressure gradients are weak, usually associated with anticyclones that have their center over southwestern Europe. In such conditions, local factors predominate and nights are calm, with possible intense cooling in valleys and plains. Fog, dew or frost could appear. This study analyzes, through the application of some selection filters, the characteristics of stable nights during the period of 1997-2005 in the agrometeorological station of Gimenells, located in the eastern half of the Ebro basin. It shows the typical evolution of wind, humidity and temperature in stable conditions, identifying its principal directions and relating them to the topography of the Ebro basin.

Key words: Stable boundary layer, conditional climatology, Lleida

1 Introduction

The Ebro basin is an approximately triangular shaped valley, oriented on the NW/SE axis, ca. 400 km long, closed in by some important mountain ranges (the Pyrenees and Cantabrian Mountains to the north, Iberian System to the west and south and Pre-coastal Catalan Range to the East). The outflow to the sea goes through narrow gorges that communicate the Lleida area with the coastal area, and for this reason the basin could be considered, in a primary approximation, a closed valley (Figure 1). The valley has a slope to the SE following its main axis, and the lateral slopes converge to the center from the Pyrenees, the Iberian System and the Catalan Pre-coastal Range, configuring a bucket where the lower areas are located between Zaragoza and Lleida, with the lowest and widest area close to Lleida.

This topographic configuration makes the climatology in the Ebro basin different from the surrounding areas. Winds blowing from the west usually arrive dry after crossing the several ranges located in the interior of the Iberian Peninsula and are channelled following the valley axis. Winds from the north and south must go around the Pyrenees and also take the direction of the valley. In the case of winds blowing from the north, a mesoscale low pressure area is generated downwind and the channelled wind is locally called *Cerç* or *Mestral* (Masson and Bougeault, 1996). In synoptic anticyclonic conditions with a weak pressure gradient on the area, winds are weak in wide areas of the basin, often generated at slopes during the night, converging in the valleys and plains, with areas of cold air accumulation where fog and frost can occur. Some examples of similar dynamics have been documented in other places, such as the Mesa Creek Valley in the state of Colorado (Gudiksen et al., 1992) or the Hudson River Valley (Fitzjarrald and Lala, 1989).

As the central valley and the Lleida region are areas mainly dedicated to agrarian production with some important population centers, it is important to have a good knowledge of climatic behavior on stable nights, which could create some significant problems for the population (due to fog formation or little dispersion of atmospheric pollution) or for the agriculture (due to frost formation). It is especially important to study the temperature behavior in such situations, since important falls in this variable could entail intense frosts (Snyder and de Melo Abreu, 2005). Previous studies have dealt with the risk of frosts in the Ebro basin (Hernandez Navarro, 1995) or have elaborated a general cli-

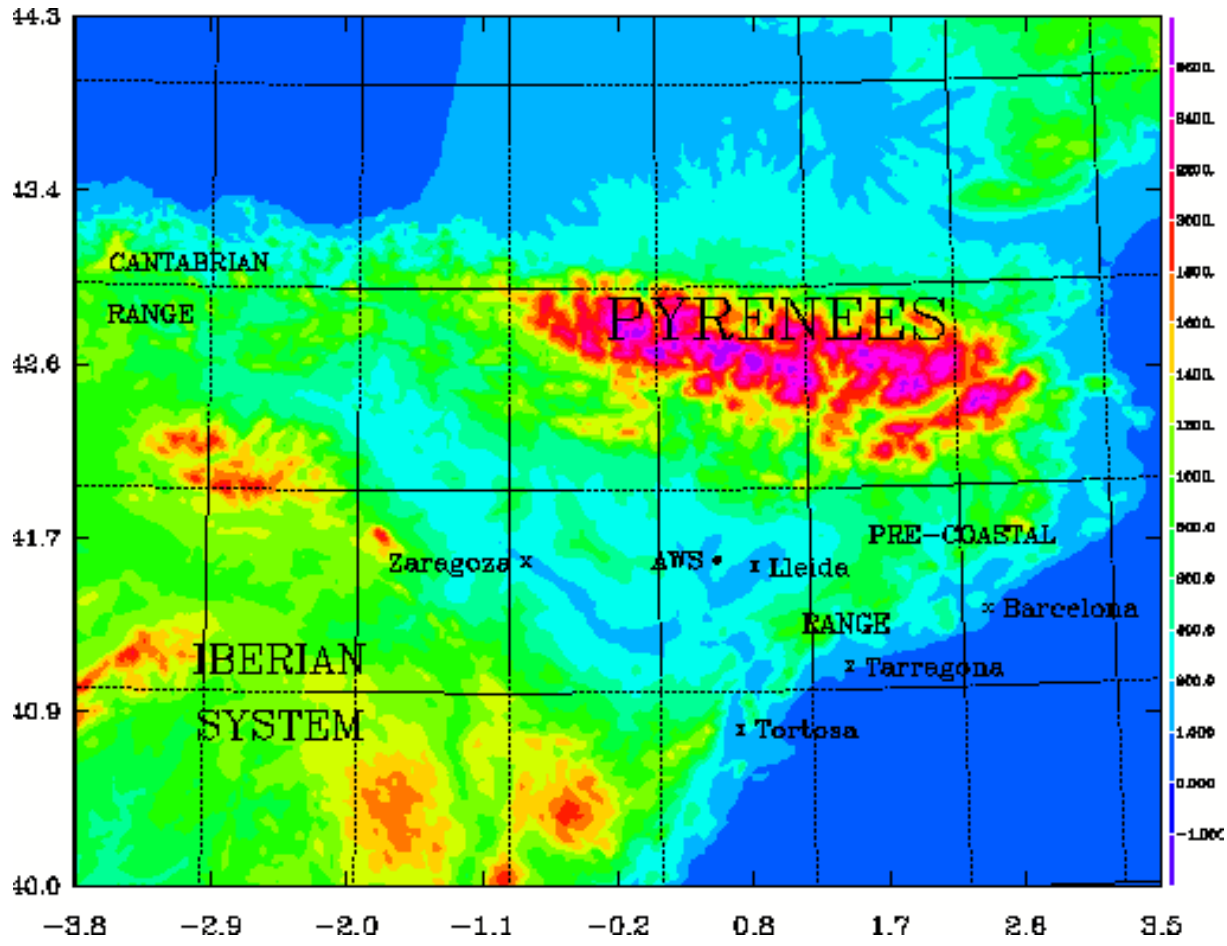

Figure 1. Location of the Gimenells AWS in the Ebro basin.

matology for Lleida city (Sousa, 1987). However, as far as the authors know, there is still no climatic study conditioned to stable nights in the area, nor have they found it for any other place.

The study of the climate of an area is usually done by using statistical parameters of the principal meteorological variables. The characterization of some episodes is done according to the method of case studies, and it often combines the analysis of observations (*in situ* and remote) and simulations with mesoscale models (Cuxart et al., 2007). While climatology describes the average behavior of the weather in a certain area and gives information about the variability of the studied series, the case studies describe situations which can appear regularly (as it is the case of anticyclones when local effects predominate) or sporadically.

A case study does not have, in principle, statistical representativity. To be considered representative, it is first necessary to study the climatology of the area of interest conditioned to the situation to be studied, and check if the selected case behaves consistently with the correspondent conditioned climatology. This study aims to characterize stable nights in the Ebro basin, more precisely in the Lleida area, in order to, in subsequent studies, evaluate if a determined case study is representative of the behavior indicated by the climatology.

Accordingly, it is necessary to develop a study methodology of climatic series conditioned to the existence of particular meteorological situations. To be specific, those that are favorable to the development of local circulations are typically related to weak pressure gradients in an area. This will allow studying the characteristics of stable nights from a statistical point of view.

In the absence of relevant synoptic gradients, the heterogeneity of the surface (due to topography or to the uses of the soil) favors the appearance of phenomena such as drainage flows, valley winds, breezes or cold pool growth (Whiteman, 1990) that strongly condition meteorological measurements and make possible the appearance of significant differences between stations which are close to each other (Cuxart et al., 2007).

In section 2 the environment of the weather station chosen for this study is described. The station is located in the Segrià (the region around Lleida), in a relatively homogeneous area (regarding crops and topography) and far away

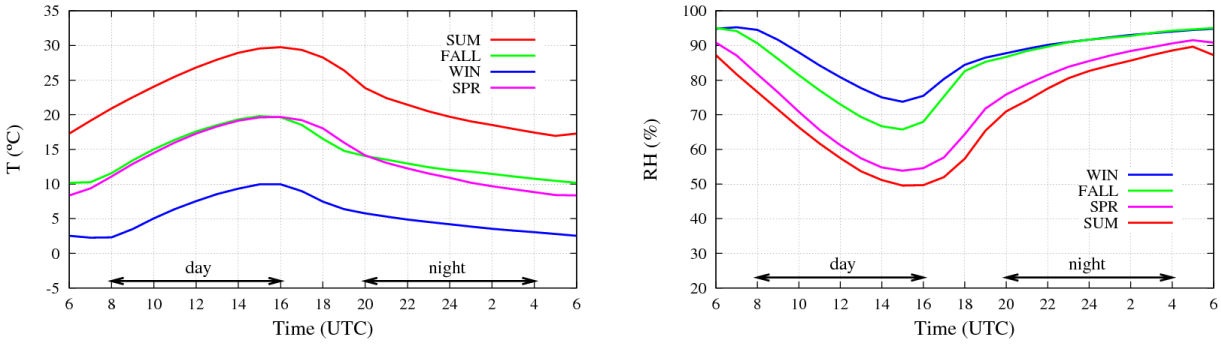

Figure 2. Daily cycle of the average temperature (°C, left) and relative humidity (%, right) for all four seasons calculated from the time series registered in the Gimenells AWS in the period 1997-2005.

from any important population centers. There is as well climatic information from the main Lleida station, located in the same area. A 9-year series of hourly data will be studied, described in section 3, only for the stable nights with weak wind, no clouds or fog, as they are the most favorable to the development of local circulations and at a hydrographic basin scale.

In section 4, three factors to filter the series are defined using the information provided only by the station, based on insolation, relative humidity and wind speed. After that, in section 5, the filtered series are analyzed, the physical significance of the results in both local dynamics and basin terms is discussed, and the validity of the methodology is evaluated. Finally, in section 6 the most relevant conclusions are given. In the future, it is expected to test this methodology simultaneously in several stations in the same basin.

2 Climatology and location

The automatic weather station (AWS) of Gimenells (0.394°E, 41.656°N) is located 248 m above sea level (ASL), on the western side of the Lleida area. From a physiographic point of view, the station is on a plateau located between the rivers Cinca and Segre, in the eastern part of the Ebro basin, with the Pyrenees to the north and the Pre-coastal Range to the east (Figure 1). The basin stretches to the west with several tributaries of the Ebro river coming from the Pyrenees (the Cinca and the Gàllego, among others), the river Jalón being the main tributary from the right side, which brings water from the Iberian System.

The station is located 20 km to the west of Lleida (which is 155 m ASL) and 25 km to the north of where the Ebro and its tributaries Cinca and Segre meet at 128 m ASL. The area is locally plain, but it is on a basin slope oriented from north to south and from east to west with a very weak slope. The Central Pyrenees are in the north, with peaks higher than 3000 m ASL, together with the pre-Pyrenees, a group of mountains located between the main rivers (Segre, les Nogueres, Éssera and Cinca) that are oriented from west to east, the closest ones of which are the Montsec (1677 m ASL, 50 km to the Northeast) and the Serra Llarga (509 m ASL, 25 km to the north). The layout of these mountains favors katabatic flows to be mainly channeled along the river valleys.

The Pre-coastal Range borders the basin on its eastern and southeastern edges to the Ebro River. To the east, the maximum elevations of the different ranges are between 700 and 900 m ASL, with a very gentle slope, without any important obstacles to the west, passing Cervera and Tàrrega (548 and 373 m ASL respectively) to the Pla d'Urgell (ca. 250 m ASL average). To the southeast, the mountains lose elevation, from the highest ones (Prades and Montsant, that are ca. 1200 m ASL in height), to those on the border of the plain, which are approximately 500-600 m ASL in height. On the southern side of the Ebro, the Iberian Mountains present a complex relief with heights ca. 400 m ASL when passing by the Ebro, that increase until 1470 m ASL over Ports de Beseit, at a distance of 100 km.

It is to be expected that this topographic distribution highly conditions the climatology of the studied area, as it has already been observed in a numerical study of air circulations in Mallorca Island in similar meteorological circumstances (Cuxart et al., 2007). The drainage flows generated in the mountains located in the area between the east and south do not encounter any significant orographic obstacle and, in principle, can arrive well developed over the Lleida area.

The entire region is characterized by an intense agrarian activity. Next to the station there is an experimental crop area (42 ha of fruit trees, cereals and fodders) and, in the surrounding areas, there are fields of cereal, vegetables and fruit trees. To the northeast there are irrigation lands (corn, alfalfa) and at 4 km to the northeast, the wine-growing region of Raimat (2245 ha).

From a climatic point of view, the Lleida area is one of the driest in Catalonia, with a pronounced continental climate. In the Lleida station of the *Agencia Estatal de Meteorología* (AEMET) (Spanish meteorology agency), accord-

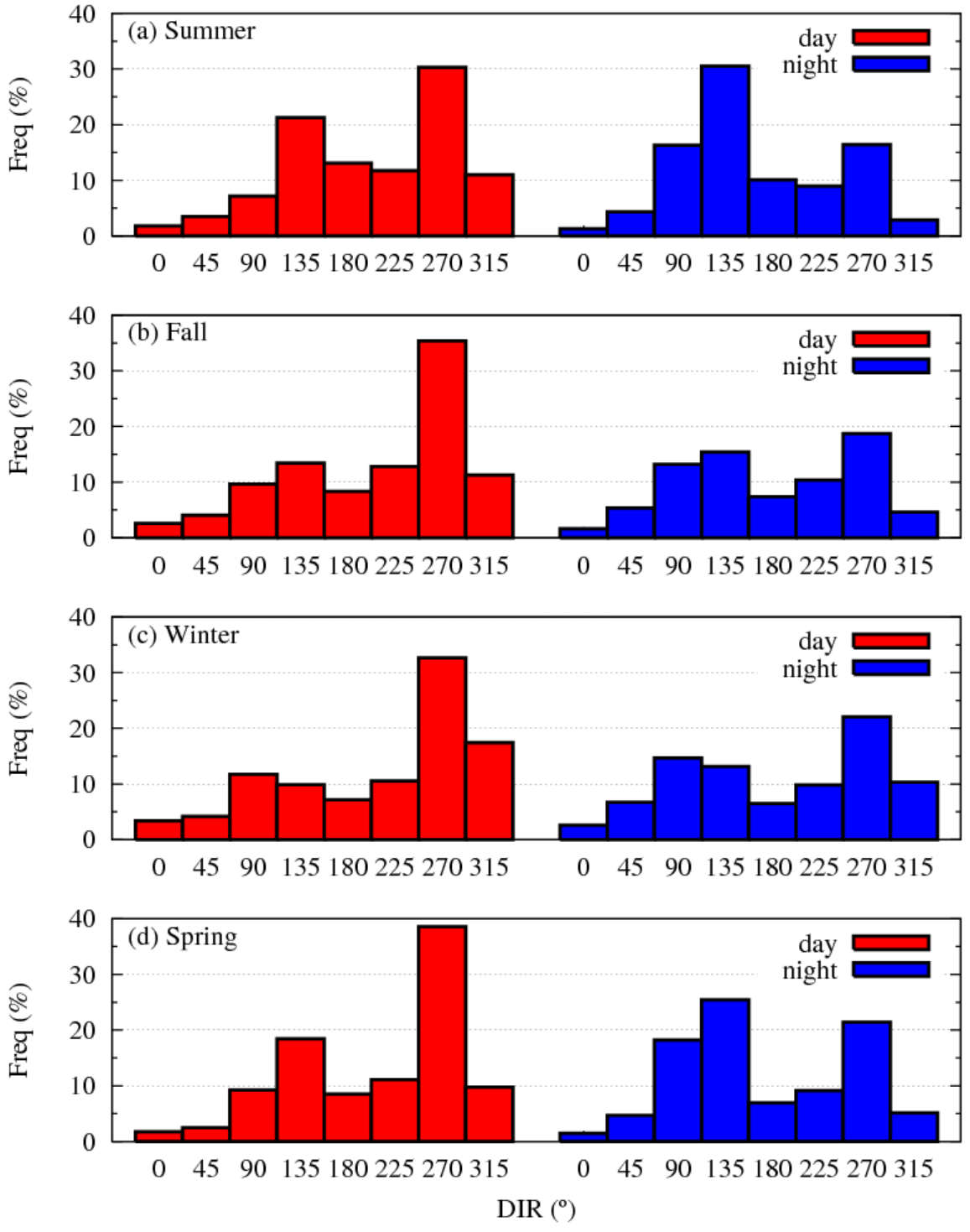

Figure 3. Frequency distribution (%) of wind direction (°) for the seasons of (a) summer, (b) fall, (c) winter, and (d) spring, calculated from the time series registered in the Gimenells AWS in the period 1997-2005. The day corresponds to the hourly data obtained from the period 08 - 16 UTC and the night, from the period 20 - 04 UTC (see Figure 2).

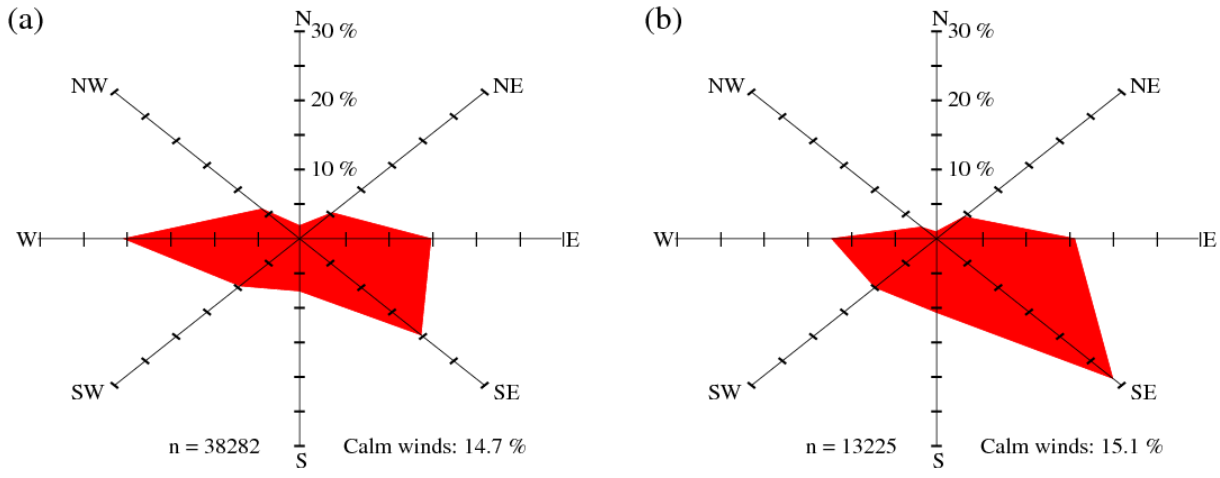

Figure 4. Wind rose for all (a) nights, and (b) stable nights according to the criteria defined in the text (Formula 4). Winds are considered calm when the wind speed has an hourly average inferior to 0.2 m s^{-1}. n indicates the number of data used for each diagram.

ing to their website[1], for the period of 1971-2000, the average precipitation was 369 mm per year, with maximum values in spring and fall, with an average yearly temperature of 14.7°C and a yearly thermal range of 20°C (the difference between the average temperature of the warmest and the coldest months). These are characteristics of a continental Mediterranean dry climate (Martín-Vide, 2005). There are 46 days with rainfall over 1 mm, 53 days of fog (37 between November and January) and 37 days of frost. Fog could be persistent in the area during winter anticyclones, remaining over the area 24 hours a day. Average maximum temperatures are over 30°C in summer and the average minimum is 1°C in winter. The extreme values in Lleida were 41.2°C on July 30th 1983 and -14.2°C on January 8th 1985.

3 Characteristics of the temporal series

The station of Gimenells belongs to the *Xarxa d'Estacions Meteorològiques Automàtiques* (XEMA) (Automatic Weather Stations Network), of the *Servei Meteorològic de Catalunya* (SMC) (Meteorological Service of Catalonia) and it is located in the municipality of Gimenells and el Pla de la Font, about 600 m away of the town of Gimenells. The *Departament d'Agricultura, Ramaderia i Pesca* (DARP) (Department of agriculture, farming and fishing) of the Catalan government set up this installation on December 1st 1996 for agrometeorological purposes. It measures (i) the temperature at 1.5 m above ground level (AGL), (ii) wind speed and direction at 2.0 m AGL, (iii) relative humidity at 1.5 m AGL, (iv) global solar radiation and (v) precipitation.

[1]http://www.aemet.es/en/elclima/datosclimatologicos/valoresclimatologicos?l=9771C\&k=cat

Until March 2005, temperature and relative humidity data were taken with a sampling frequency of 10 minutes whereas samples in the fields of wind, rainfall and solar radiation were taken every second. The hourly data saved were the scalar average of the sample values for one hour. From April 2005, the data (not considering rainfall) is taken with a sampling frequency of one per second in order to calculate minute averages (in the case of wind speed and direction these are vectorial averages, according to the normative UNE500520). In this work, hourly averages for the period 1997-2005 have been used (taken from the minute averages for the interval April-December 2005).

For the studied time interval, the quality control of SMC was based on filling in the blanks of the series by using a linear interpolation when there is a period of one or two hours. In all other cases, the series is left untouched. Throughout these nine years of data compilation there have been blanks concentrated in two periods: (i) from 08 UTC on August 6th 1999 to 00 UTC on September 4th of the same year and (ii) from 04 UTC to 10 UTC on June 8th 2003. As the number of missing data represents less than 1% of the total, these points in the series are not considered in the following analysis.

Figure 2 shows the daily cycle of the average temperature and relative humidity for all four seasons, taken from the temporal series of 9 years. Related to temperature, transition seasons (fall and spring) have very similar evolution and values. The average amplitude is ca. 10°C and night temperatures are slightly lower in spring, when there is less fog and night cooling can be more intense at the end of the night. Winter has the smaller daily thermal amplitude (ca. 7°C) and the minimum absolute night cooling, even if temperatures are clearly below the other seasons, while summer is the season with a wider daily thermal amplitude

13°C). Relative humidity also shows a very clear daily cycle for all seasons. Values shortly after midday show that spring and summer have values below the average (60%) while in fall and winter values are about 10 to 25% higher. During the night, all seasons register very high values of relative humidity due to strong superficial radiative cooling.

Figure 3 shows the distribution of wind speed frequencies during 9 years of data for each season. To distinguish the relevant directions during day and night, calculations have been made for the periods 08 - 16 UTC and 20 - 04 UTC, respectively, therefore avoiding the influence of the variation in the time of sunrise and sunset along the year. During the day, wind from the W predominates in all seasons. The explanation is that this is an area with general winds from the W and so these are predominant if there is no anticyclone.

On the other hand, by night there is a approximately bimodal distribution, with maximum from the W and E/SE. The first ones could also be related to general circulation; while the second ones could be produced by the generation of drainage flows from mountains located in these directions and relatively nearby. However, it must be noted that wind from the N and NE is rare in this AWS, despite the presence of the Pyrenees and Montsec mountains in these directions, and everything seems to indicate that this is a phenomenon linked to the peculiarities of the circulation in the area (the channelling of these low-level winds by the Segre and Cinca valleys, as observed in other complex basins (Gudiksen et al., 1992)).

4 Selection of stable nights

It is very difficult to distinguish the specific climatic characteristics of stable nights, based on the general climatology of an AWS, which are strongly conditioned by local circulation. In order to make a more accurate analysis, the current study has developed a method to select stable nights from the series based on the variables measured at the station.

The goal is to detect the nights of the series with clear skies and a weak synoptic pressure gradient. Unfortunately, the Gimenells AWS has no net radiation sensor (which could indicate if there is strong cooling and therefore clear skies) that allows identifying the nights that have these characteristics. There is also no pressure sensor, even if this measure itself does not allow the estimation of the gradient (stationary pressures could have strong winds associated). However, and despite the difficulties, it has been decided to build a simple selection method from the information obtained from the analyzed AWS in order to generalize it to other stations.

In this study, the specifically defined parameters to extract the nights of interest are:

$$Q_d = \frac{Q_t - Q_e}{Q_t} \tag{1}$$

$$HUM = \frac{HR_d - HR_s}{HR_d} \tag{2}$$

$$\overline{V_n} = \frac{1}{N}\sum_{N} v_i \tag{3}$$

The first (Q_d) is named *insolation deficit index*, where Q_t and Q_e represent the theoretically and measured average daily insolation, respectively. It calculates the difference between measured solar radiation and the radiation that theoretically arrives to the top of the atmosphere at the same latitude and day of the year. Therefore, besides the dimming effect of the bulk of the atmosphere, the other reason for this difference is the cloudiness during the day. Actually, on a cloudy day, the value of Q_d will be higher than on a sunny day. With this index it is assumed that the cloudiness during daylight time is similar to that produced during the following night. This parameter allows ruling out the days with cloudiness of a synoptic origin, associated to fronts or disruptions and that, due to the temporal scale of the phenomenon, does often affect the following night as well. However, there are situations in which Q_d could discriminate cloudy days of strictly daily evolution (cumulus) typical of good weather and followed by a stable night. This condition has been considered when defining the threshold value of this parameter.

HUM is the *index of the humidity cycle*. It uses average relative humidity (HR_d) and average relative humidity measured only during daylight (HR_s). It depends on the daily cycle of relative humidity. If this is important, the average relative humidity during daylight hours would be lower than daily relative humidity, therefore producing a HUM value higher than if the relative humidity is relatively constant throughout the day. Large daily cycles of temperature and humidity involve great contrasts between day and night, a situation often found in stable conditions. Relative humidity has been used instead of temperature because one of the aims of this study is to analyze the evolution of this variable on stable nights. Therefore, it was decided not to use it as a discriminating factor.

On the other hand, HUM discards atmospheric situations with meteorological phenomena of a temporal scale that are longer than a day (dry advections, for instance), as well as situations of persistent fog throughout the day. As indicated in section 2, persistent fog is a winter phenomenon that is frequent in the area, which significantly disturbs the balance of energy on the surface as it changes the quantity of net radiation that reaches the surface; those cases were discarded in the current study.

Finally, $\overline{V_n}$ is the *average speed of night wind*, where v_i represents wind speed at the i-hour of the night. It is used to discard the nights with an important synoptic or mesoscalar pressure gradient, which can be translated into a moderate wind close to the surface.

Stable nights are considered to be those that comply of the following inequalities:

$$Q_d \leq 0.4; \quad HUM \geq 0.07; \quad \overline{V_n} \leq 2\, ms^{-1} \tag{4}$$

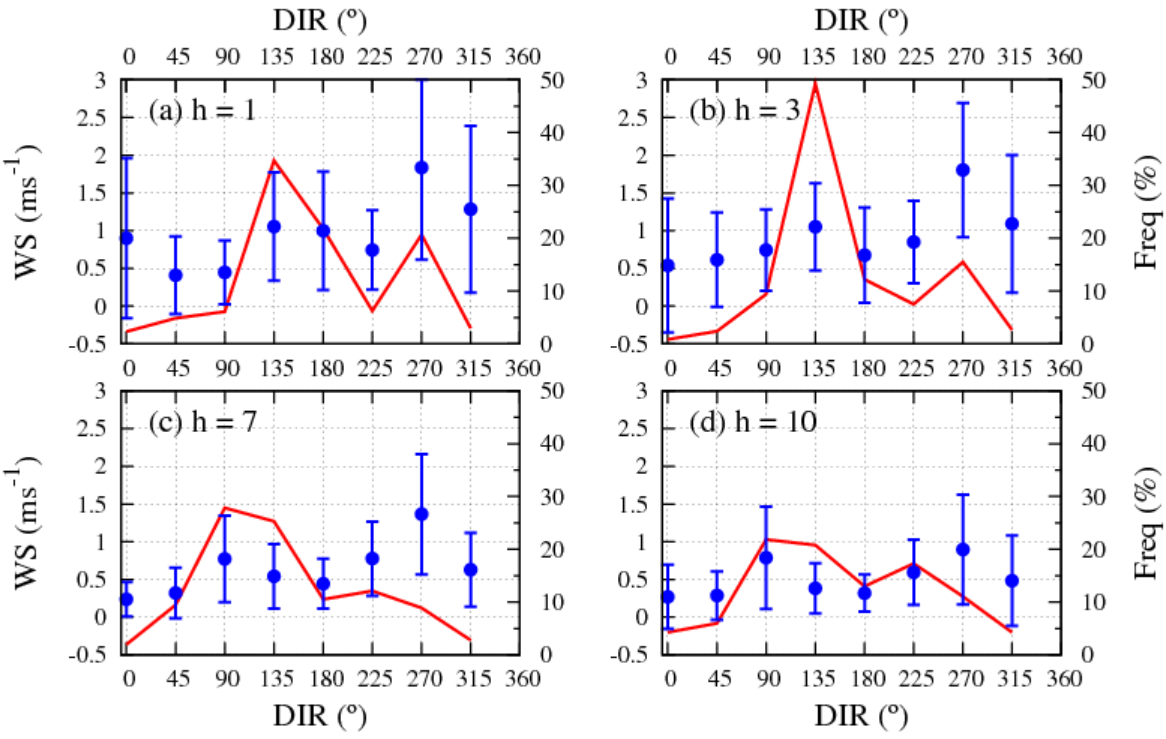

Figure 5. Average wind speed (m s^{-1}) regarding the direction (°) (blue) and frequencies distribution (%) of the wind direction (red) for the (a) first, (b) third, (c) seventh and (d) tenth night hours. The night hours refer to the number of hours from the last registered data before sunset. Error bars indicate the standard deviation of the group of individual results that contribute to the wind average value.

All the nights with an average wind speed below 2 m s^{-1}, preceded by a day with little cloudiness and dry in relation to the night will be selected.

The threshold values are selected as follows. On the one hand, the limit of Q_d considers those days when measured average global radiation represents at least, 60% of what theoretically arrives to the top of the atmosphere. On an clear sunny day, Q_d value is greater than 0.2, while when a front passes, Q_d exceeds 0.6.

The fixed threshold for HUM is small because this is a parameter that has values between 0.00 and 0.20 for the vast majority of nights. For instance, HUM value is lower than 0.09 on a day that has had the same daily oscillation as the average represented in summer (Figure 2). Therefore, the selected value includes cases with a daily oscillation of, at least, the average obtained during that season.

The restriction imposed on the average speed of the night wind is based on previous experimental studies. During the experimental campaign of SABLES98 (Cuxart et al., 2000), that took place on the Duero basin, stable situations had wind speeds below 2 m s^{-1} close to the ground. Actually, Conangla and Cuxart (2006) impose a similar criterion for the selection of nights with a maximum of well-defined wind at low-level jet. Among other restrictions, wind average every 30 minutes at 2.2 m AGL should be lower than 2 m s^{-1}. In that study, all selected nights corresponded to synoptic situations defined by a strong anticyclone with its center next to the Iberian Peninsula. In the current study, this condition is less rigidly applied, as it is the average of the hourly wind measured along the night, which has to be under the established value limit.

Table 1. Number of stable nights in the 9 year series for each season (left) and percentages regarding the total number of nights of the time series (center) and regarding the season (right).

	n. of stable nights	% over the total	% over season total
WINTER	125	10.3	15.5
SPRING	380	31.3	45.9
SUMMER	447	36.8	54.8
FALL	262	21.6	32.2
Total number	1214	100	37.3

When applying this filter, 1214 stable nights are obtained out of a total of 3253. Table 1 shows the number of cases according to the season, summer being the one with a higher absolute number of nights that fulfill the required conditions (and there is nearly one month of the summer of

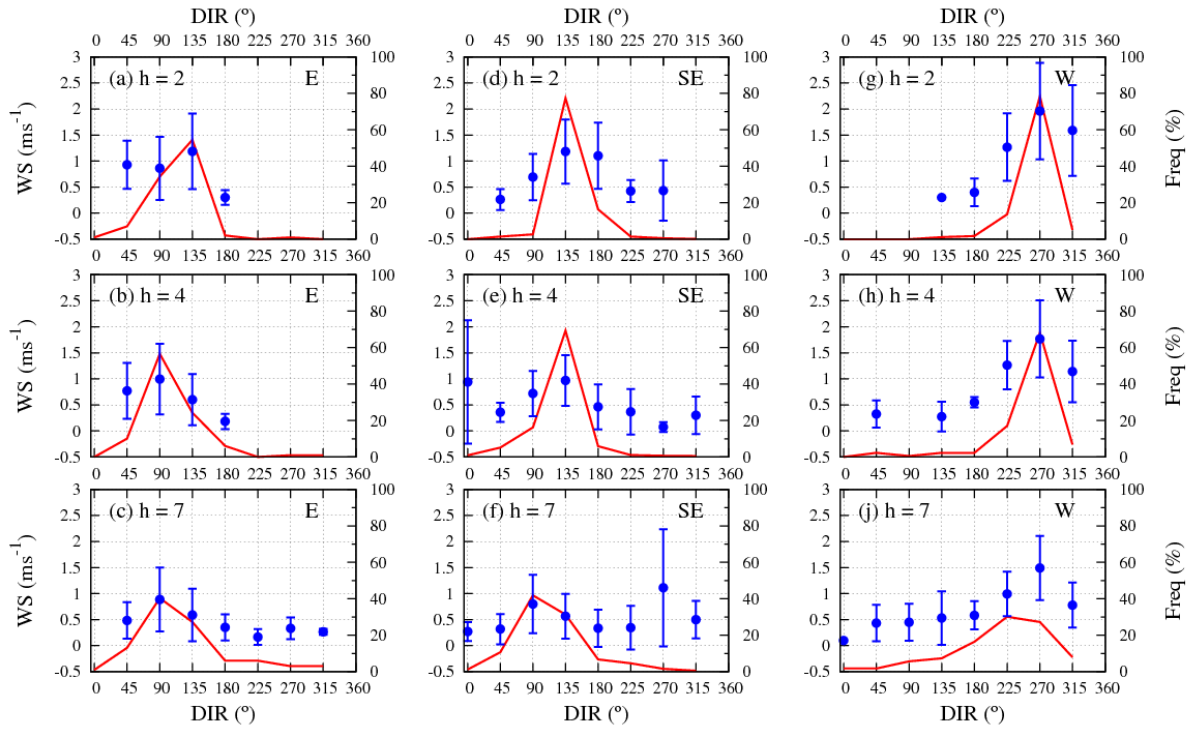

Figure 6. Same as Figure 5 but with stable nights gathered in three different subgroups, according to wind direction during the third night hour (Figure 5b): (i) E (left column), (ii) SE (central column) and (iii) W (right column) for (a, d, g) second, (b, e, h) fourth and (c, f, j) seventh night hours.

1999 missing in the series). The following is spring, over fall, when fog is more frequent and its likeliness is lower in winter, as in these months there are frontal passages combined with anticyclones that generate persistent fog. The percentages elaborated for each season show that approximately half of the nights in the summer and spring fit the given definition of stable nights, while these proportions decline to 32% and 16% in fall and winter, respectively.

5 Study of the selected nights

5.1 Wind roses and nightly evolution

Figure 4 compares the wind roses of the total number of nights and of the subgroup of selected nights. The general rose shows three predominant directions (W, E and SE with ca. 20% each) and a little represented sector (NE and NW with ca. 5% and N with 2%). The rose, during stable nights, has its main sector to the SE (28%) and the E (15%), W frequency descends to 12% and N sector is still rare. It can be observed that the proportion of calms[2] is similar in both roses (15%), which indicates that there are situations of weak wind that do not fulfill the required criteria. Nights with persistent fog could be an example. Moreover, assuming that the cloudiness of the day will remain during the night, it is possible to have cloudy nights after a cloudy day, which would also explain the persistence of the proportion of calm nights.

The diminishing of west winds on stable nights is the result of filtering situations of west winds with associated cloudiness and cases of strong Cerç winds. The predominance of SE winds indicates a probable influence of high mountains located in that direction (Prades, Montsant) and winds from the E could indicate slope winds from the Segarra plateau. Instead, drainage flows from sector N, which could come from the Pyrenees or Montsec, do not arrive to the weather station in significant quantities, possibly because they descend channeled by the nearby valleys of Segre and Cinca, as indicated in the climatologies of the stations located next to the Segre River (available at www.meteo.cat). It must be noted that recent numeric studies (Cuxart et al. (2007) for Mallorca, Bravo et al. (2008) for the Duero basin indicate that nocturnal drainage flows are organized and interact, and this could explain circulations that seem apparently counterintuitive.

In order to inspect the evolution of the wind direction frequency distribution during the night, attention will be focused on four significant moments (Figure 5): (i) beginning of the night, (ii) change of tendency, (iii) late night and (iv) end of the night. In the first hour SE predominates, with high percentages of S and W. In the third hour, the SE pre-

[2]It is considered calm when the hourly average of the wind speed is lower than 0.2 m s^{-1}.

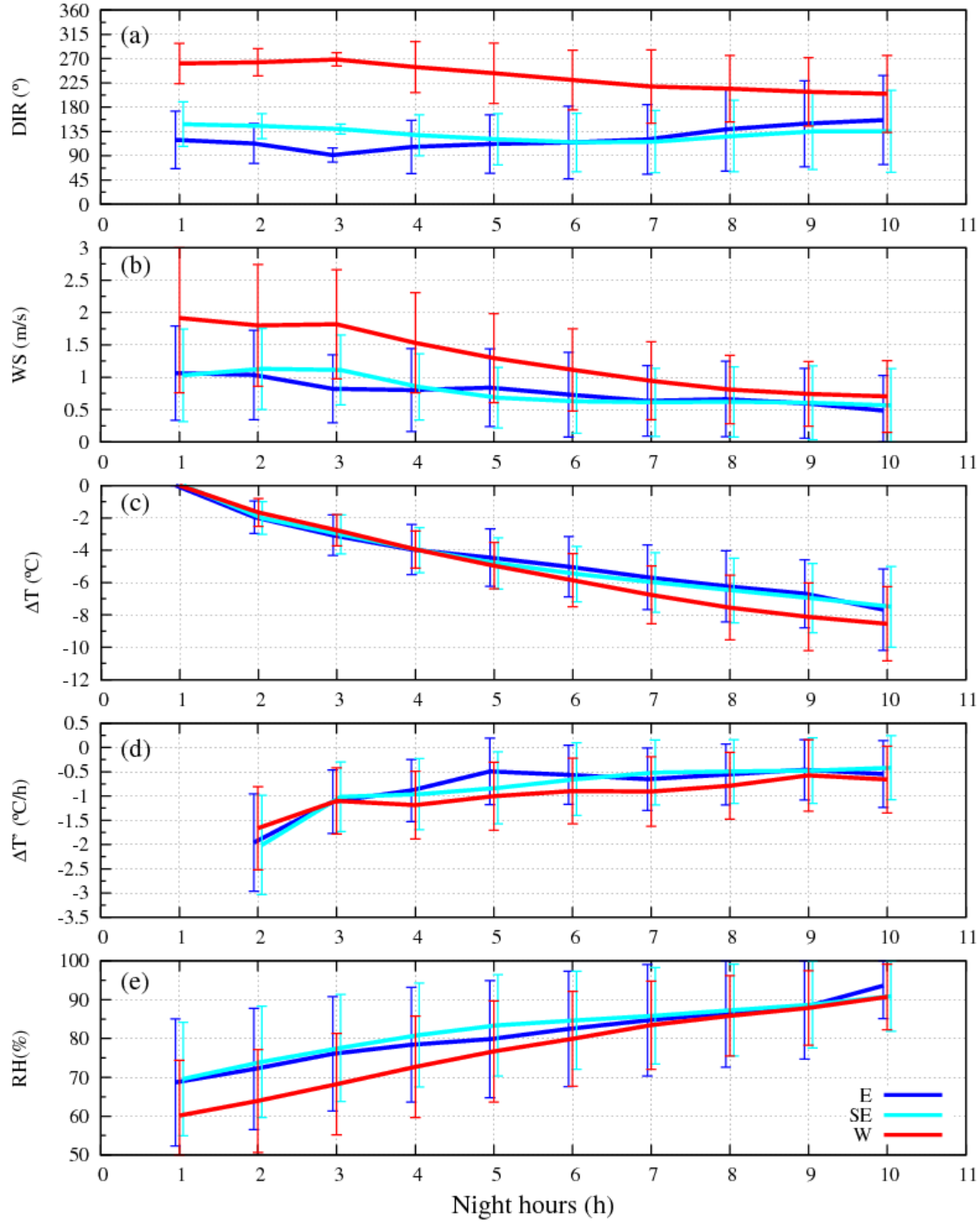

Figure 7. Temporal evolution of the average of wind (a) direction (°) and (b) speed (m s^{-1}), (c) cooling (°C), (d) cooling hourly rate (°C h^{-1}) and (e) relative humidity (%) for all three subgroups of stable nights defined in Figure 6. The bars indicate standard deviation. The abscissa axis corresponds to the hour of the night (defined in Figure 5).

dominance has increased (it gets to its maximum value during the night) and S and W descend to relatively low values that will be maintained during the whole night, while the E component is increased in the final hours of the night as SE decreases gradually, until it is exceeded in the seventh hour. Calm winds are more frequent at the end of the longest nights, between the end of fall and beginning of spring (not shown). The amount of data decreases after the seventh hour due to the shorter length of the night in summertime.

Trying to make a reading of these statistics in a physical code is risky. One could think that at the first hour there could be either (i) winds from the W of one type (weak west winds), or (ii) a local winds linked to weak pressure gradients that favor winds from the S and the SE that turn to the E during the night, linked to the topography of this part of the basin. Actually, when analyzing on an hourly basis, it is evident that the night distribution is bimodal, there is more frequency of SE or E at all hours, with W/SW being the second most frequent with winds that usually have twice the strength as in the first case (Figure 5).

To evaluate this hypothesis, three subgroups were chosen out of all the nights selected, defined according to the predominant direction in the third hour after sunset (Figure 5b): W (15.5%), SE (49.3%) or E (9.3%). This instant was selected because the time of the night when there is the maximum data concentration in a specific direction (SE). By doing a similar analysis to this one for all nights, but paying attention to the instants immediately prior and after the hour chosen to divide the three subgroups, one could see that the evolutions of E and SE are very similar, and the case of E could be considered as one of the cases that have changed faster than the others (Figure 6a - 6f). Both of them show the SE component in the first hours of the night turning to E between 4 and 6 hours after sunset.

Instead, nights with wind from the W three hours after sunset keep this direction as predominant during the rest of the night with a gradual diminishing of speed as the night goes on (Figure 6g - 6j).

5.2 Temperature, speed and humidity evolution

Figure 7 shows the evolution of some variables for each subgroup above defined, giving the curve that links average values and standard hourly deviations. The subgroups from E and SE have similar behaviors, which suggests a similar origin for both cases (drainage flows). It can be observed that the evolution of the direction is very different depending on wind direction during the third night hour. There are fewer differences at the end of the night, when the wind speed is smaller in both cases. In fact, the average speed is nearly double on the nights when the wind blows from the W than when it blows from E/SE.

Thermal evolution shows similar coolings in all three cases during the first five hours. Since this moment, if the winds regime is W, the air gets cooler than if it blows from the E/SE. It is still not clear if this difference is due to the different nature of the phenomena that intervene in each of the mentioned regimes. The cooling per hours is more intense in the first part of the night (2°C h^{-1} at the beginning and 1.5°C h^{-1} thereafter) and gets stable in the second part with values of 0.5°C h^{-1} in the case of drainage and slightly higher for west winds (0.7°C h^{-1}). Snyder and de Melo Abreu (2005) highlight that those nights with frost risk have similar behaviour, with very intense coolings around sunset (that could reach 10°C h^{-1} in some cases) and smoother at the end of the night (1°C h^{-1}). Regarding relative humidity, west winds start at the beginning of the night with values an average of 10% lower than when the wind blows from E/SE. However, in all cases, relative humidity is increased during the night with the diminishing of temperatures reaching an average values of 90%, which generates dew and mist or fog at the end of the night.

Figure 8 shows, on the other hand, the same variables (except wind direction) for all selected nights grouped by seasons. The most remarkable thing in this figure is that there are no qualitative differences between the evolution during the different seasons. The curves are almost parallel to each other, and the only difference is their length, due to the variation in the number of night hours depending on the season. In all of them, the wind speed decreases in the middle of the night, humidity increases to values close to saturation and cooling eight hours after sunset is 6 to 7 degrees with similar error bars. Hourly cooling also follows the same pattern, with intense cooling during the first hour of the night (2°C h^{-1}), moderate between the third and the seventh (between 1.5 and 1°C h^{-1}) and gentle in the last period (lower than 1°C h^{-1}). This perseverance in the behavior of the main meteorological variables allows for the predefinition of a night evolution pattern for the Gimenells AWS, regardless of the season.

6 Conclusions

With the objective of characterizing the average behavior of the meteorological variables of the Gimenells AWS, conditioned to some specific characteristics on calm nights with weak wind, three parameters have been defined. These parameters made it possible to extract nights of interest just by using the data registered in the station for the years 1997-2005. Insolation, relative humidity and wind speed were used as discriminative variables, leaving aside temperature as its behavior is of special interest during stable nights.

The chosen parameters seek out nights that correspond to days with a well defined daily cycle and weak winds on the station (until to 2 m s^{-1} a 2 m AGL). The filters selected 37.3% of the nights in the 9 years series, which indicates a first estimation of the frequency of this kind of weather in the Lleida area (clear nights with weak or calm winds and no fog). They occur mainly in the summer and spring, as in the fall and winter this situation normally generates fog and the nights are not selected. As fog is a protective factor against steep temperature drops, clear and calm nights are the most likely to cause frosts. In the Gimenells AWS these nights

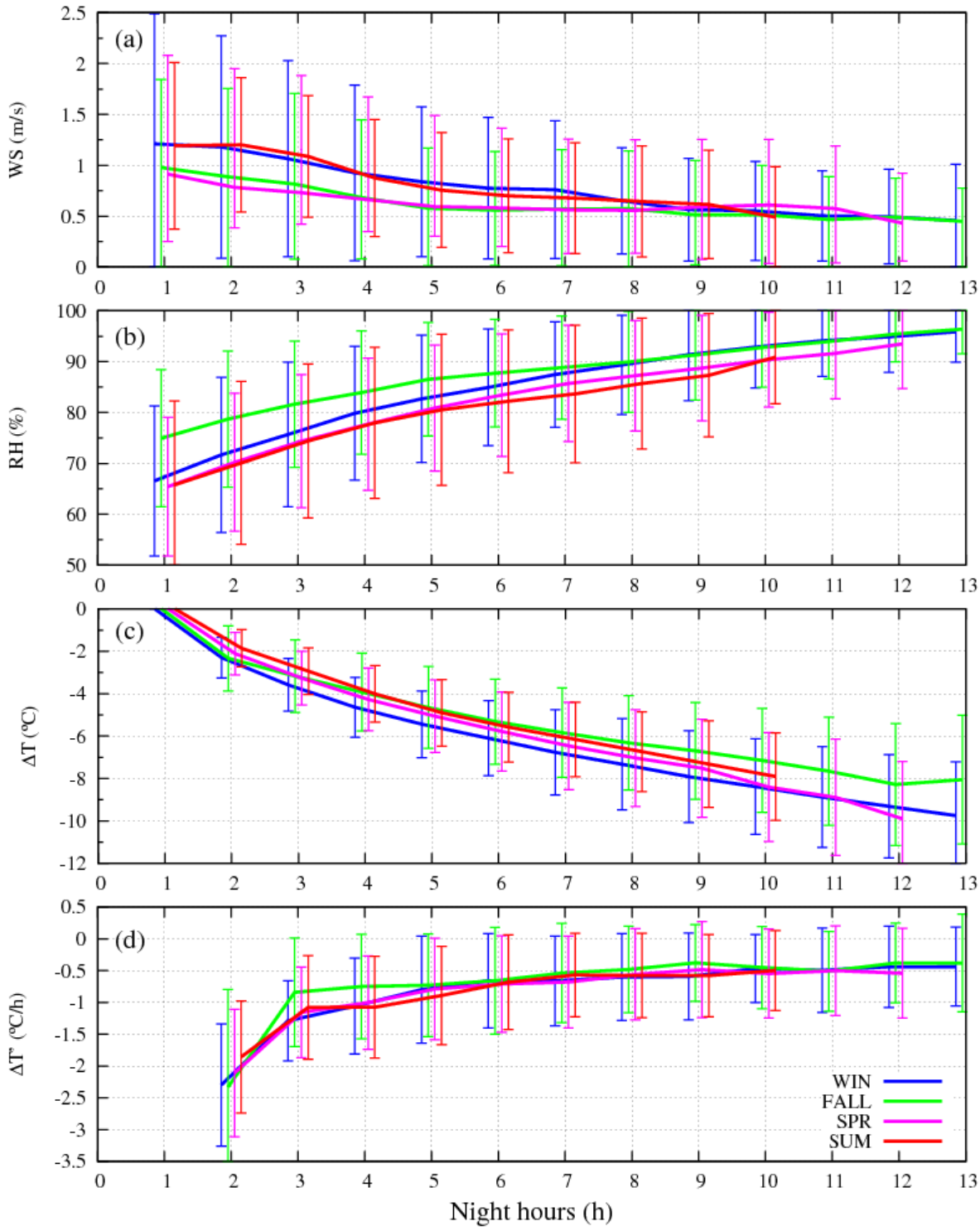

Figure 8. The same as Figure 7 for the variables (a) wind speed (m s^{-1}), (b) relative humidity (%), (c) cooling (°C) and (d) hourly cooling rate (°C h^{-1}) for all four seasons: winter (WIN), spring (SPR), fall (FALL) and summer (SUM) for all selected nights.

represent up to 16% of all nights in the winter and a 46% of the spring nights, which is the most critical season for agriculture.

The study of the wind shows that there are two kinds of preferential regimes in the selected station. The first and more usual one seems to be related with drainage flows that are first generated in the SE, in the ranges of Prades and Montsant and arrive later on from the E from the Segarra plateau. The second in frequency is a regime of weak west winds, which maintain their direction during the whole night. Winds from the north sector do not arrive well defined to the station and this could be due to its channeling through the valleys of Segre and Cinca that, as they are power in respect to the station, would be under the drainages described above. In any case, the observed winds always tend to decrease during the night.

The temperature drop follows a unique pattern for all regimes and stations. Cooling during the four hours after sunset is ca. 4°C, while during the first eight nightly hours the temperature descends ca. 8°C in the case of west winds, and 6.5 °C when there are drainage flows. In all cases, there is a strong hourly cooling (2°C h^{-1}) in the first hour after sunset, which declines gradually as the night draws on. These results make it possible to estimate the minimum temperature regarding the measured temperature just after sunset and the winds regime.

To confirm what the study indicates, other observatories in the area must be explored, especially those with longer climatic series, to see if there are any congruent conclusions, as well as to carry out studies with a numeric and experimental character that confirm the hypothesis developed here.

Acknowledgements. This work has been possible thanks to the funding of the research project CGL2006-12474 and the grant FPI BES-2007-16272, from the MEC. The manuscript has been enriched by the suggestions of Dra. Maria Antònia Jiménez and some calculations done by Felipe Molinos. We would also like to acknowledge the collaboration of Tomeu Clapés in the design of Figure 1 and the comments of Mr. Miquel Perpinyà i Romeu, from the SMC, about data quality control, as well as the comments of two anonymous reviewers.

References

Bravo, M., Mira, T., Soler, M. R., and Cuxart, J., 2008: *Intercomparasion and evaluation of MM5 and Meso-NH mesoscale models in the stable boundary layer*, Bound-Lay Meteorol, **128**, 77–101.

Conangla, L. and Cuxart, J., 2006: *On the Turbulence in the Upper Part of the Low-Level Jet: An Experimental and Numerical Study*, Bound-Lay Meteorol, **118**, 379–400.

Cuxart, J., Yagüe, C., Morales, G., and Terradellas, E., 2000: *Stable Atmospheric Boundary-Layer Experiment in Spain (SABLES 98): A report*, Bound-Lay Meteorol, **96**, 337–370.

Cuxart, J., Jiménez, M., and Martínez, D., 2007: *Nocturnal Meso-Beta and Katabatic Flows on a Midlatitude Island*, Mon Wea Rev, **135**, 918–932.

Fitzjarrald, D. R. and Lala, G. G., 1989: *Hudson valley fog environment*, J Appl Meteorol, **28**, 1303–1328.

Gudiksen, P. H., Leone, J. M. J., King, C. W., Ruffieux, D., and Neff, W. D., 1992: *Measurements and modelling of the effects of ambient meteorology on nocturnal drainage flows*, J Appl Meteorol, **31**, 1023–1032.

Hernandez Navarro, M. L., 1995: El riesgo de helada en las plantaciones de frutales. El valle medio del Ebro, Institución "Fernando el Católico", Zaragoza, 237 pp.

Martín-Vide, J., 2005: Factors geogràfics, regionalització climàtica i tendències de les sèries climàtiques a Catalunya, J. E. Llebot, Institut d'Estudis Catalans, Barcelona, informe sobre el canvi climàtic a Catalunya, pp. 81-111.

Masson, V. and Bougeault, P., 1996: *Numerical simulation of a low-level wind created by complex orography: a Cierzo case study*, Mon Wea Rev, **124**, 701–715.

Snyder, R. and de Melo Abreu, J., 2005: Frost protection: fundamentals, practice and economics, Service Series 10, FAO, Roma, environment and natural resources, Vol. 1, 240 pp.

Sousa, R., 1987: Notas para una climatología en Lérida, K-26, Instituto Nacional de Meteorología, Madrid.

Whiteman, C. D., 1990: Observations of thermally developed wind systems in mountainous terrain, W. Blumen, Amer. Meteor. Soc. Boston, atmospheric Processes over Complex Terrain, Meteor. Monogr., volume 23, pp. 5-42.